Arabidopsis Sphingolipid Fatty Acid 2-Hydroxylases (AtFAH1 and AtFAH2) Are Functionally Differentiated in Fatty Acid 2-Hydroxylation and Stress Responses[1][OA]

Minoru Nagano, Kentaro Takahara, Masaru Fujimoto, Nobuhiro Tsutsumi, Hirofumi Uchimiya, and Maki Kawai-Yamada*

Graduate School of Biological Science, Nara Institute of Science and Technology, 8916–5 Takayama, Ikoma 630–0101, Japan (M.N.); Institute of Molecular and Cellular Biosciences, University of Tokyo, Bunkyo-ku, Tokyo 113–0032, Japan (K.T.); Graduate School of Agricultural and Life Sciences, University of Tokyo, Bunkyo-ku, Tokyo 113–8657, Japan (M.F., N.T.); Graduate School of Science, University of Tokyo, Bunkyo-ku, Tokyo 113–0033, Japan (M.F.); Institute for Environmental Science and Technology (H.U., M.K.-Y.) and Department of Environmental Science and Technology (M.K.-Y.), Saitama University, Sakura-ku, Saitama 338–8570, Japan; and Iwate Biotechnology Research Center, Kitakami, Iwate 024–0003, Japan (H.U.)

2-Hydroxy fatty acids (2-HFAs) are predominantly present in sphingolipids and have important physicochemical and physiological functions in eukaryotic cells. Recent studies from our group demonstrated that sphingolipid fatty acid 2-hydroxylase (FAH) is required for the function of Arabidopsis (*Arabidopsis thaliana*) Bax inhibitor-1 (AtBI-1), which is an endoplasmic reticulum membrane-localized cell death suppressor. However, little is known about the function of two Arabidopsis FAH homologs (AtFAH1 and AtFAH2), and it remains unclear whether 2-HFAs participate in cell death regulation. In this study, we found that both AtFAH1 and AtFAH2 had FAH activity, and the interaction with Arabidopsis cytochrome b_5 was needed for the sufficient activity. 2-HFA analysis of *AtFAH1* knockdown lines and *atfah2* mutant showed that AtFAH1 mainly 2-hydroxylated very-long-chain fatty acid (VLCFA), whereas AtFAH2 selectively 2-hydroxylated palmitic acid in Arabidopsis. In addition, 2-HFAs were related to resistance to oxidative stress, and AtFAH1 or 2-hydroxy VLCFA showed particularly strong responses to oxidative stress. Furthermore, AtFAH1 interacted with AtBI-1 via cytochrome b_5 more preferentially than AtFAH2. Our results suggest that AtFAH1 and AtFAH2 are functionally different FAHs, and that AtFAH1 or 2-hydroxy VLCFA is a key factor in AtBI-1-mediated cell death suppression.

Sphingolipids are a large class of lipids present ubiquitously in eukaryotic cells and involved in various cellular processes such as signal transduction, protein transport, and programmed cell death as structural components of the plasma membrane and tonoplast and as signaling molecules (Dunn et al., 2004; Pata et al., 2010). These numerous functions are based on the structural diversity of sphingolipids. Complex sphingolipids are largely formed by a variety of head groups and a ceramide, which is comprised of a long-chain base amide linked to a fatty acid. One of the main characteristics of sphingolipid fatty acids is that large number of sphingolipids contained very-long-chain fatty acids (VLCFAs; fatty acids with ≥ C20; Raffaele et al., 2009). Another feature is the 2-hydroxylation of fatty acids (Alderson et al., 2005). The 2-hydroxy fatty acid (2-HFA)-containing sphingolipids are present in most organisms, including yeast (*Saccharomyces cerevisiae*), vertebrates, and plants. Especially in higher plants, 2-HFAs are contained in more than 90% complex sphingolipids such as glucosylceramides and glycosylinositolphosphorylceramides (Imai et al., 1995; Pata et al., 2010).

The 2-hydroxylation of sphingolipid *N*-acyl chains is catalyzed in yeast and mammals by the enzyme sphingolipid fatty acid 2-hydroxylase (ScFAH1 and FA2H, respectively, and we refer to them as FAH in this report; Mitchell and Martin, 1997; Alderson et al., 2004; Hama, 2010). FAH is an endoplasmic reticulum (ER)-localized membrane protein composed of two domains: an N-terminal cytochrome b_5 (Cb5)-like domain and a putative catalytic site with the His motif (HXXHH), which coordinates the nonheme diiron cluster at the active site of the enzyme and is highly conserved among membrane-bound desaturases and hydroxylases. Mammalian FA2H is reported to catalyze

[1] This work was supported by a Research Fellowship for Young Scientists of Japan Society for the Promotion of Science (to M.N.), a Grant-in-Aid for Scientific Research for Plant Graduate Student from Nara Institute Science and Technology (to M.N.), and a grant from the Japan Society for the Promotion of Science through the Funding Program for Next Generation World-Leading Researchers (NEXT Program), initiated by the Council for Science and Technology Policy.

* Corresponding author; e-mail mkawai@mail.saitama-u.ac.jp.

The author responsible for distribution of materials integral to the findings presented in this article in accordance with the policy described in the Instructions for Authors (www.plantphysiol.org) is: Maki Kawai-Yamada (mkawai@mail.saitama-u.ac.jp).

[OA] Open Access articles can be viewed online without a subscription.

www.plantphysiol.org/cgi/doi/10.1104/pp.112.199547

the 2-hydroxylation of free fatty acid in vitro, which was dependent on a reconstituted electron transport system (Alderson et al., 2005). In mammals, FA2H-synthesized 2-HFAs abundantly accumulate in epidermal keratinocytes and the myelin-forming cells of the nervous system (Alderson et al., 2006; Uchida et al., 2007; Maldonado et al., 2008). Loss of *FA2H* in mouse altered the composition and physicochemical properties of sebum, causing alopecia (Maier et al., 2011). In addition, FA2H deficiency also causes a wide range of neurodegeneration phenotypes such as spastic paraplegia, leukodystrophy, and brain ion deposition (Schneider and Bhatia, 2010). Moreover, FA2H is a negative regulator of the cell cycle and facilitates dibutyryl-cyclic AMP-induced cell cycle exit in D6P2T schwannoma cells (Alderson and Hama, 2009). These studies suggest that 2-hydroxylation of fatty acids is important in various cellular functions in mammals. However, there had been few reports about plant FAHs in the past.

Recently, we suggested that FAH could mediate the function of Bax inhibitor-1 (BI-1), which is an ER membrane-localized cell death suppressor widely conserved in animals and plants (Xu and Reed, 1998; Kawai-Yamada et al., 2001; Nagano et al., 2009). Arabidopsis (*Arabidopsis thaliana*) BI-1 (AtBI-1) plays important roles in the resistance to various biotic and abiotic stresses including pathogens, ER stress, ion stress, and oxidative stress generating reactive oxygen species (ROS; Kawai-Yamada et al., 2001, 2004, 2009; Watanabe and Lam, 2006, 2008; Ihara-Ohori et al., 2007; Ishikawa et al., 2010). Our recent work indicated that AtBI-1 interacted with ScFAH1, and that deletion of *ScFAH1* prevented AtBI-1 from suppression of cell death induced by mammalian proapoptotic protein, Bax, in yeast cells (Nagano et al., 2009). In Arabidopsis, there are two highly identical FAH homologs, AtFAH1 and AtFAH2, which possess several His motifs like their yeast and mammalian counterparts. However, AtFAH1 and AtFAH2 lack a Cb5-like domain, which provides electrons to ScFAH1 and FA2H (Mitchell and Martin, 1997; Alderson et al., 2004; Nagano et al., 2009). Instead, we demonstrated the interaction between both AtFAHs and Arabidopsis Cb5s (AtCb5s), which are localized in the ER membrane or mitochondrial outer membrane, by using a split-ubiquitin yeast two-hybrid system. In addition, AtBI-1 also interacted with AtCb5s. Moreover, overexpression of *AtBI-1* increased the amounts of 2-hydroxy VLCFAs. These results allowed us to speculate that AtBI-1 interacts with AtFAHs via AtCb5 to activate the synthesis of 2-hydroxy VLCFA in Arabidopsis, which leads to the suppression of cell death. However, it remains unclear whether 2-hydroxy VLCFA is related to the regulation of cell death or stress responses. Furthermore, little is known about the function of AtFAH1 and AtFAH2 in 2-HFA synthesis of plant cells.

The results of this study confirmed that both AtFAHs are FAHs, and identified functional differences between AtFAH1 and AtFAH2 in fatty acid 2-hydroxylation in Arabidopsis. In addition, AtFAH1 modified the resistance to oxidative stress more strongly than AtFAH2, which was consistent with the preferential interaction with AtBI-1.

RESULTS

AtFAH1 Also Interacts with AtCb5-B in the ER of the Plant Cells

We showed previously that AtFAH2 is localized in the ER (Nagano et al., 2009). To investigate whether AtFAH1 has the same function as AtFAH2 or not, we first confirmed the subcellular localization of AtFAH1. Fusion constructs of *AtFAH1* were generated using genes encoding *GFP* driven by the cauliflower mosaic virus 35S (CaMV35S) promoter. When bombarded in onion (*Allium cepa*) epidermal cells, AtFAH1-GFP was localized in the cell periphery, the perinuclear region, and the reticulum network (Fig. 1, A and D). In addition, AtFAH1-GFP was colocalized always with AtFAH2-RFP (Fig. 1, A–C), suggesting that AtFAH1 also localizes in the ER.

As described above, neither AtFAH1 nor AtFAH2 has any Cb5-like domains (Mitchell and Martin, 1997; Nagano et al., 2009). Alderson et al. (2004) demonstrated that the Cb5-like domain is essential for human FA2H activity, implying that AtFAH1 and AtFAH2 require an ER-localized AtCb5 to increase their activity. In fact, we have already demonstrated that both AtFAH1 and AtFAH2 interacted with all ER-localized AtCb5 in yeast cells. In addition, the interaction between AtFAH2 and AtCb5-B, which is one of four ER-type AtCb5s, was reported in plant cells using a fluorescence resonance energy transfer (FRET) analysis (Nagano et al., 2009). Accordingly, we attempted to verify the interaction between AtFAH1 and AtCb5-B in plant cells by using a bimolecular fluorescence complementation (BiFC) assay. The nYFP-pUGW0 vector contains nYFP (1–174 amino acids) in the N-terminal side of the target proteins, driven by CaMV35S promoter, whereas the cYFP-pUGW2 vector contains cYFP (175–239 amino acids) in the C-terminal side (Nakagawa et al., 2007; Fig. 1E). When nYFP-AtCb5-B and AtFAH1-cYFP were transiently coexpressed in onion epidermal cells, we observed BiFC fluorescence that was highly localized in the cell periphery and the perinuclear regions (Fig. 1, F and L). This signal was similar to that of nYFP-AtCb5-B/AtFAH2-cYFP in terms of localization and intensity (Fig. 1, F, H, L, and N). In contrast, no fluorescent signal was visible using empty vectors (nYFP/cYFP; Fig. 1J). In these studies, DsRed driven by CaMV35S promoter was used as an expression marker of particle bombardment (Fig. 1, G, I, K, M, and O). These results suggest that not only AtFAH2 but also AtFAH1 interacts with AtCb5-B in plant cells.

AtFAHs Exhibit FAH Activity in Yeast Cells

To clarify whether AtFAH1 and AtFAH2 are FAHs, we performed a complementation test using yeast *ScFAH1*-deletion variant (Δ*fah1*), which cannot produce any 2-HFAs. In these experiments, *AtFAH1* or *AtFAH2*

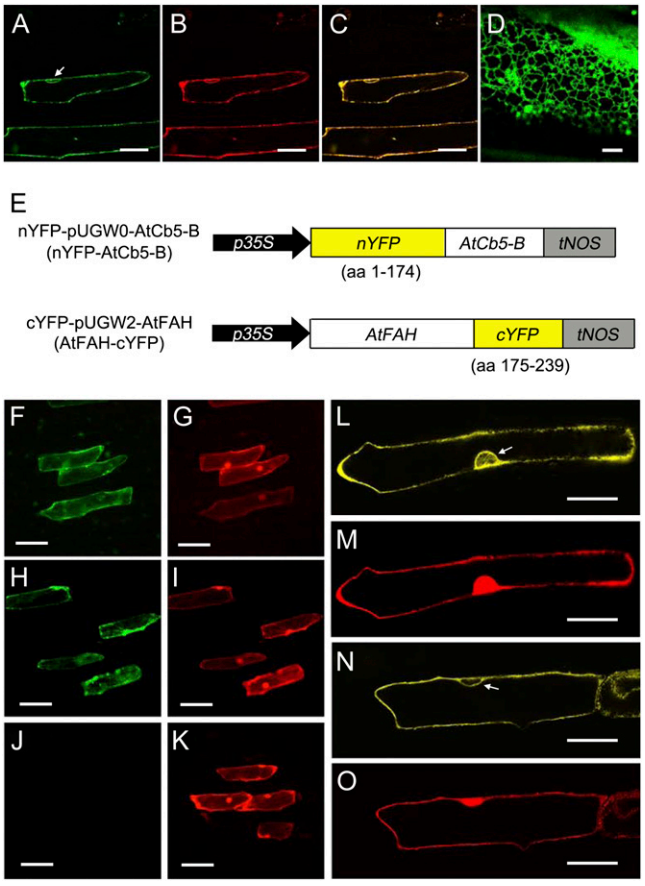

Figure 1. AtFAH1 interacts with AtCb5-B in the ER of plant cells. A to D, Distribution of AtFAH1-GFP (A and D) and AtFAH2-RFP (B). Onion epidermal cells transiently coexpressing AtFAH1-GFP and AtFAH2-RFP were examined by confocal laser-scanning microscopy. The merged images of A and B are shown in C. Scale bars in A, B, and C = 100 μm. Scale bar in D = 5 μm. Arrow indicates the perinuclear region. E, Schematic representation of BiFC constructs. The coding regions of AtCb5 and AtFAH1 or AtFAH2 were fused with the N-terminal (nYFP; 1–174 amino acids) and the C-terminal (175–239 amino acids) region of YFP, respectively. *p35S*, CaMV 35S promoter; *tNOS*, terminator of the nopaline synthase (NOS) gene. F to O, BiFC visualization in onion epidermal cells with AtFAH1-cYFP/nYFP-AtCb5-B (F and L), AtFAH2-cYFP/nYFP-AtCb5-B (H and N), and cYFP/nYFP (J). G, I, K, M, and O are CaMV35S-DsRed images as expression marker of particle bombardment of F, H, J, L, and N, respectively. F to K, Images were examined by fluorescence microscopy. L to O, Images were examined by confocal laser microscopy. Scale bars = 100 μm. Arrows in A indicate the perinuclear region.

was transformed into Δ*fah1*, and total lipids were extracted using the Folch method described previously (Folch et al., 1957). 2-HFA methyl esters were fractionated by thin-layer chromatography (TLC) after derivatization of fatty acids, and were detected by gas chromatography-mass spectrometry (GC-MS). In this assay, 2-hydroxy hexacosanoic acid (26h:0) was evaluated as a marker of 2-HFAs, because 26h:0 occupied almost all 2-HFAs in yeast (Oh et al., 1997).

As shown in Figure 2, 26h:0 accumulated in *AtFAH1*- or *AtFAH2*-expressing Δ*fah1*, but not in Δ*fah1*, suggesting that both AtFAH1 and AtFAH2 have FAH activity. However, these levels were quite less than those of the wild type and Δ*fah1* expressing *ScFAH1* (Fig. 2). This finding may be due to the structural difference between ScFAH1 and AtFAHs with or without Cb5-like domain, respectively (Mitchell and Martin, 1997; Nagano et al., 2009). Transformation of *AtCb5-B* into *AtFAH1*- or *AtFAH2*-expressing Δ*fah1* resulted in a marked increase in the amounts of 26h:0 (Fig. 2). AtCb5-B itself exhibited no FAH activity, because no 26h:0 was detected in *AtCb5-B*-expressing Δ*fah1* (Fig. 2). These results indicate that AtCb5 is a key factor for the activity of AtFAH1 and AtFAH2.

Different Roles for AtFAH1 and AtFAH2 in 2-HFA Synthesis in Arabidopsis

To elucidate the roles of AtFAH1 and AtFAH2 in 2-HFA synthesis pathway and the physiological functions in Arabidopsis, we searched for *AtFAH*s knockout lines. However, no suitable T-DNA insertion line for *AtFAH1* is available among the existing T-DNA mutant collections. We therefore generated *AtFAH1* knockdown transgenic lines (AtFAH1-KD) by RNA interference with 100 bp of 3′ untranslated region in *AtFAH1* cDNA as a trigger (Fig. 3A). Reverse transcription (RT)-PCR analysis confirmed that *AtFAH1* was markedly reduced in AtFAH1-KD-1 and -2 lines (Fig. 3C). In contrast, we obtained T-DNA-tagged Arabidopsis line in *AtFAH2* gene (SALK_011293, *atfah2*), which has a T-DNA insertion in third exon (Fig. 3B). As shown in Figure 3C, not only the full-length *AtFAH2* mRNA (primer a-b), but also the upstream region of T-DNA insertion site in *AtFAH2* gene (primer a-c) was completely deleted. AtFAH1-KD and *atfah2* plants showed no apparent phenotype compared with the 3-week-old wild-type (Columbia-0) plants under normal growth condition (Fig. 3D).

We first dissected 2-HFA composition in these transgenic plants. Total lipids including total sphingolipids were extracted from the aboveground parts in 3-week-old plants according to Markham et al. (2006), and these 2-HFA methyl esters were detected with GC-MS after derivatization. In this study, we analyzed five major 2-HFAs (16h:0, 22h:0, 24h:0, 24h:1, and 26h:0) of 13 2-HFAs in Arabidopsis (Imai et al., 2000).

In the AtFAH1-KD lines, the levels of 22h:0, 24h:0, and 26h:0 were considerably lower than in wild type, whereas the level of 16h:0 was marginally decreased (Fig. 4, A and B). In contrast, the level of 16h:0 was markedly reduced by 22.9% in *atfah2* mutant, whereas the levels of other 2-HFAs were similar to those in wild type (Fig. 4, A and B). Thus, these results suggest that VLCFA is 2-hydroxylated by AtFAH1, whereas palmitic acid is 2-hydroxylated by AtFAH2 and marginally AtFAH1.

2-HFAs Are Implicated in Resistance to Oxidative Stress and 2-Hydroxy VLCFAs Respond to Oxidative Stress

Our previous report suggested that FAH is related to AtBI-1-mediated suppression of cell death (Nagano

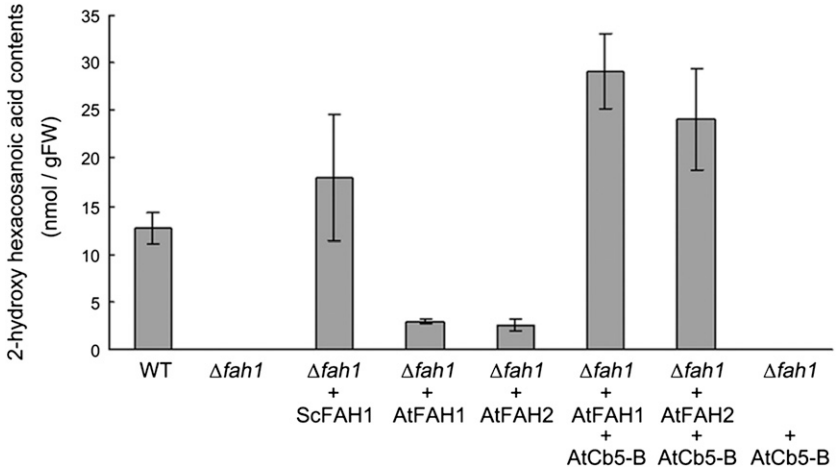

Figure 2. AtFAH1 and AtFAH2 exhibit FAH activity. Complementation test of AtFAH1 and AtFAH2. Yeast *fah1*-deletion variant was transformed with plasmids possessing *ScFAH1*, *AtFAH1*, *AtFAH2*, or *AtCb5-B*, and total lipids were extracted from each. 26h:0 methyl ester was analyzed by GC-MS. Data are mean ± SD of four experiments.

et al., 2009). Because AtBI-1 is reported to suppress oxidative-stress-induced cell death (Kawai-Yamada et al., 2004; Ishikawa et al., 2010), we tested the sensitivity of AtFAH1-KD and *atfah2* plants to oxidative stress by using ROS-inducing chemicals, hydrogen peroxide (H_2O_2), and menadione (MD; Yoshinaga et al., 2006). Treatment of leaf discs obtained from 3-week-old plants with 100 mM H_2O_2 or 60 μM MD for 24 h significantly increased electrolyte leakage in AtFAH1-KD and *atfah2* plants compared with wild type (Fig. 5A). Electrolyte leakage measurement is the assay often used to examine irreversible membrane damage by oxidative stress or during cell death. In addition, chlorophyll contents in AtFAH1-KD and *atfah2* plants were lower than wild type (Fig. 5B), indicating that AtFAH1-KD and *atfah2* plants have higher sensitivity to oxidative stress. Moreover, *AtFAH2* gene controlled by its native promoter (*pAtFAH2*::*AtFAH2*, Fig. 5C) complemented the *atfah2* phenotype for oxidative-stress-induced ion leakage and chlorophyll contents (Fig. 5, A and B). These results suggest the involvement of 2-HFAs in the resistant response to oxidative stress.

Next, the expression levels of *AtFAH1* and *AtFAH2* mRNAs in response to H_2O_2 were examined. Total mRNAs were extracted from 10-d-old wild-type plants treated with 100 mM H_2O_2 for 1, 3, 5, 7, and 24 h. RT-PCR analysis showed that *AtFAH1* mRNA increased rapidly at 1 h and subsequently remained at higher levels than no treatment, although they were decreased slightly with time (Fig. 6A). *AtFAH2* mRNA diminished gradually from 3 h and was only expressed weakly at 24 h. Incidentally, *AtBI-1* mRNA continued to increase gradually in response to H_2O_2 until 24 h. These results imply that *AtFAH1* promptly responds to oxidative stress, whereas *AtFAH2* does not.

To clarify the roles of 2-HFAs in the response to oxidative stress, we examined changes in fatty acids in response to oxidative stress. Four-week-old Arabidopsis wild-type plants were treated with H_2O_2 for 24

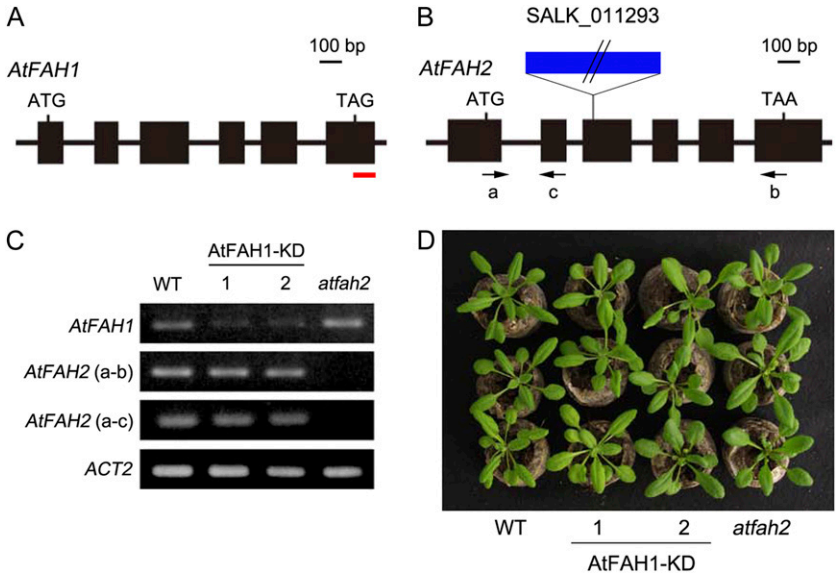

Figure 3. AtFAH1-KD lines and *AtFAH2* T-DNA insertion mutant. A, Structure of the *AtFAH1* gene. Red line represents the region which was used as a trigger of RNA interference. B, Structure of the *AtFAH2* gene and designated locations of the T-DNA. Arrows indicate the sites of primers used for PCR. C, RT-PCR analysis of *AtFAH1*, *AtFAH2* (a-b), *AtFAH2* (a-c), and *Actin 2* (*ACT2*) expression in 10-d-old seedlings of wild-type, AtFAH1-KD, and *atfah2* plants. Representative results of five experiments with similar findings. D, Phenotypes of 3-week-old AtFAH1-KD and *atfah2* plants.

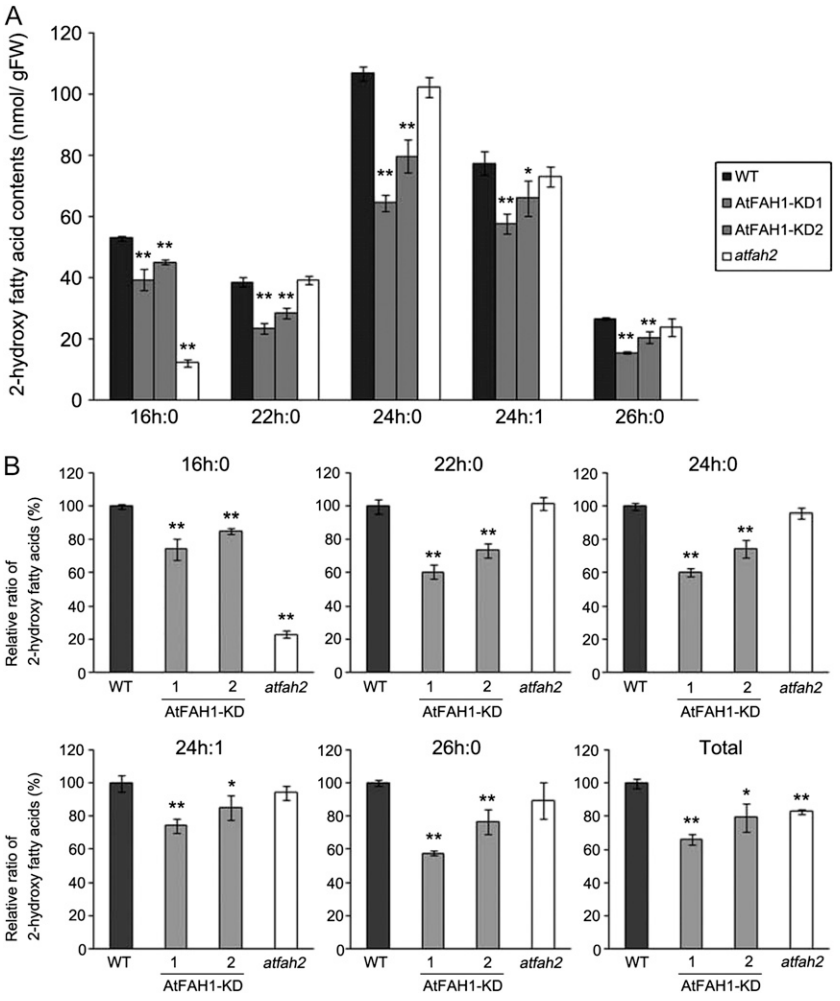

Figure 4. Quantitative analysis of 2-HFA methyl esters in AtFAH1-KD and *atfah2* plants. A, 2-HFA methyl esters were isolated from wild-type, AtFAH1-KD, and *atfah2* plants, and analyzed by GC-MS. The amounts of 2-HFAs in each sample were calculated using 2-hydroxypentadecanoic acid (15h:0) as the internal standard. B, Analysis of the relative value of each 2-HFA. Data are the relative ratios of each 2-HFA in AtFAH1-KD and *atfah2* plants. The value of each wild type was set at 100%. Data in A and B are mean ± SD of three biological replicates. $*P < 0.05$, $**P < 0.01$, compared with wild type (*t* test).

h, and their derivatized 2-HFA methyl esters and nonhydroxy fatty acid (non-HFA) methyl esters were analyzed by GC-MS. As shown in Figure 6B, the total non-HFA content was significantly lower at 24 h after treatment with H_2O_2. In contrast, total 2-HFA content was higher at 24 h after treatment with H_2O_2 (Fig. 6C). However, the amount of 16h:0 was not affected by H_2O_2 (Fig. 6D), whereas the levels of total 2-hydroxy VLCFAs were especially elevated (Fig. 6E). These results suggest the importance of 2-hydroxy VLCFAs under oxidative stress condition.

To further confirm the relationship between AtFAHs and oxidative stress, we analyzed the levels of oxidative-stress-related metabolites in the leaves of 3-week-old AtFAH1-KD and *atfah2* plants grown under normal growth conditions by using a capillary electrophoresis (CE)-MS. As shown in Figure 7, reduced glutathione (GSH) level in AtFAH1-KD was significantly lower than wild-type plants, whereas oxidized glutathione (GSSG) was markedly higher, resulting in reduced rate of GSH in total glutathione in spite of the lower total glutathione in AtFAH1-KD lines (Fig. 7, A–D). In addition, reduced ascorbate was markedly lower in AtFAH1-KD lines (Fig. 7E). Moreover, γ-aminobutyric acid (GABA) was markedly increased compared with wild-type plants (Fig. 7F). In contrast, the levels of glutathione, reduced ascorbate, and GABA in *atfah2* were similar to those in wild type (Fig. 7, A–F).

Ascorbate (vitamin C) is the most important reducing substrate for H_2O_2 detoxification in plant cells, and the series of ROS-scavenging reactions accompanied by glutathione is called the ascorbate-glutathione cycle (Nakano and Asada, 1987; Mehlhorn et al., 1996; Noctor and Foyer, 1998). When plants are exposed to ROS-mediated stresses, glutathione-ascorbate cycle participates in detoxification of ROS at the expense of electrons from the GSH pool, causing a transient increase in GSSG (Noctor and Foyer, 1998). In addition, GABA is a four-carbon nonprotein amino acid that is rapidly and markedly produced in response to biotic and abiotic stress (Kinnersley and Turano, 2000; Bouché and Fromm, 2004). Therefore, these results indicate that AtFAH1-KD lines are exposed to some stress even under nonstress conditions. Taken together, the results indicate that 2-HFAs seem important in the

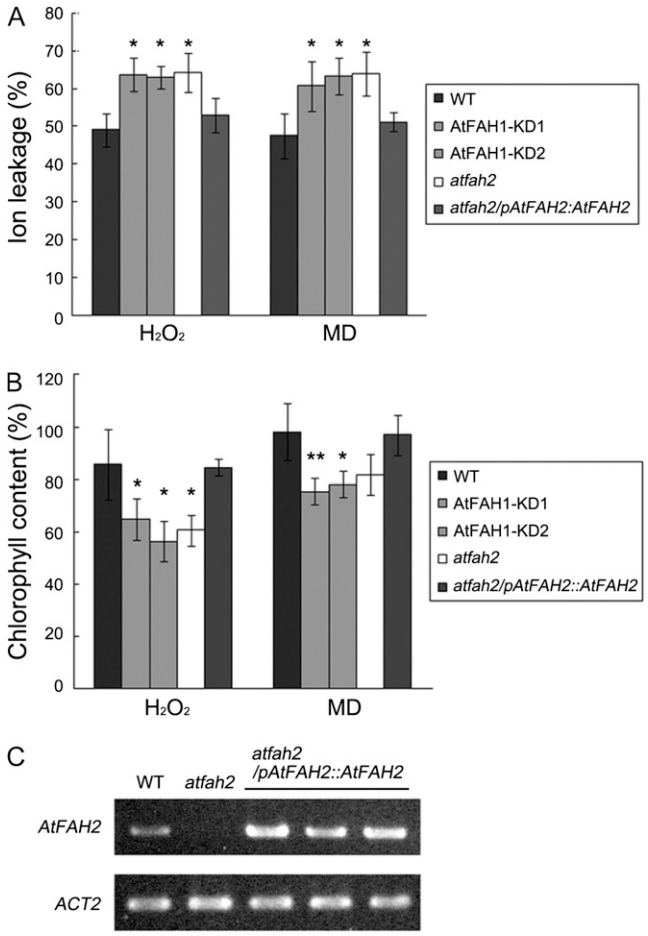

Figure 5. Sensitivity to oxidative stress in AtFAH1-KD and *atfah2* plants. A and B, Leaf discs of wild-type, AtFAH1-KD, *atfah2*, and *atfah2*/*pAtFAH2*::*AtFAH2* plants were exposed to H_2O_2 or MD for 24 or 6 h, respectively. A, Relative ratios of ion leakages to total ion. B, Relative ratios of chlorophyll contents to total chlorophyll contents. Data in A and B are mean ± SD of four biological replicates. $^*P < 0.05$, $^{**}P < 0.01$, compared with wild type (*t* test). C, RT-PCR analysis of *AtFAH2* and *ACT2* expression in 10-d-old seedlings of wild-type, *atfah2*, and *atfah2*/*pAtFAH2*::*AtFAH2* plants. Representative results of three experiments with similar findings.

plant machinery that serves to resist oxidative stress, and that the role of 2-hydroxy VLCFAs in oxidative stress response seems different from that of 16h:0.

AtBI-1 Preferentially Interacts with AtFAH1 via AtCb5-B

To reinforce the link between AtFAH and AtBI-1-mediated suppression of cell death, we examined the three-way interaction among AtBI-1, AtCb5, and AtFAH in plant cells using the BiFC-based FRET assay in plant cells. This assay detects ternary complexes in living cells by the combination of BiFC and FRET assays (Shyu et al., 2008a, 2008b; Kwaaitaal et al., 2010; Taoka et al., 2011). When the combination of AtBI-1-CFP, nYFP-AtCb5-B, and AtFAH1-cYFP, and the combination of AtBI-1-CFP, nYFP-AtCb5-B, and AtFAH2-cYFP were transiently expressed in onion epidermal cells, CFP fluorescence and BiFC signal were completely merged in both combinations (Fig. 8, A–F). We next examined the interactions between AtBI-1 and AtCb5-B/AtFAH1 or AtCb5-B/AtFAH2 by FRET-acceptor photobleaching analysis. The mean FRET efficiency was 17.4% ± 5.58% for the pair of AtBI-1-CFP and nYFP-AtCb5-B/AtFAH1-cYFP (Fig. 8G). In contrast, the pair of AtBI-1-CFP and nYFP-AtCb5-B/AtFAH2-cYFP showed a lower-level FRET efficiency (6.8% ± 2.72%), although the efficiency was significantly higher than control experiments (CFP + YFP, 3.19% ± 2.8%; Fig. 8G). These results suggest preferential ternary interactions among AtBI-1, AtCb5, and

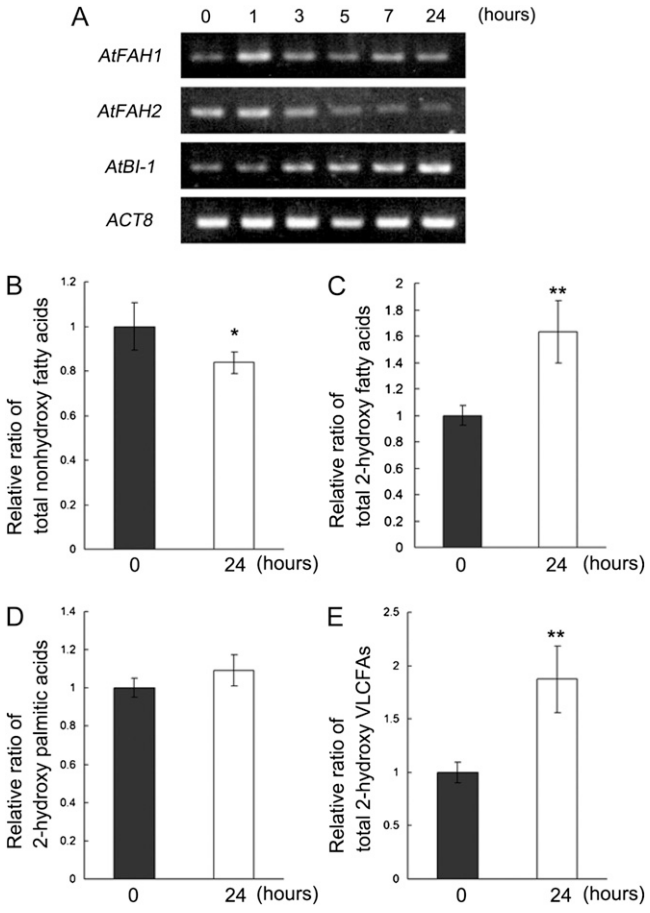

Figure 6. Analysis of mRNA and fatty acids in response to H_2O_2. A, Leaf discs of wild-type plants were exposed to H_2O_2 for 0, 1, 3, 5, 7, and 24 h, and each total RNA was extracted. The expression of *AtFAH1*, *AtFAH2*, and *AtBI-1* was analyzed by RT-PCR. Representative results of five experiments with similar findings. B to E, Non-HFAs and 2-HFAs were prepared from 4-week-old wild-type plants after treatments with H_2O_2 for 0 or 24 h. Data are the relative ratios of fatty acids in 24 h. B, Total non-HFAs. C, Total 2-HFAs. D, 2-Hydroxy palmitic acids. E, Total 2-hydroxy VLCFAs. The value of 0 h was set at 1. Data are mean ± SD of four biological replicates. $^*P < 0.05$, $^{**}P < 0.01$, compared with 0 h (*t* test).

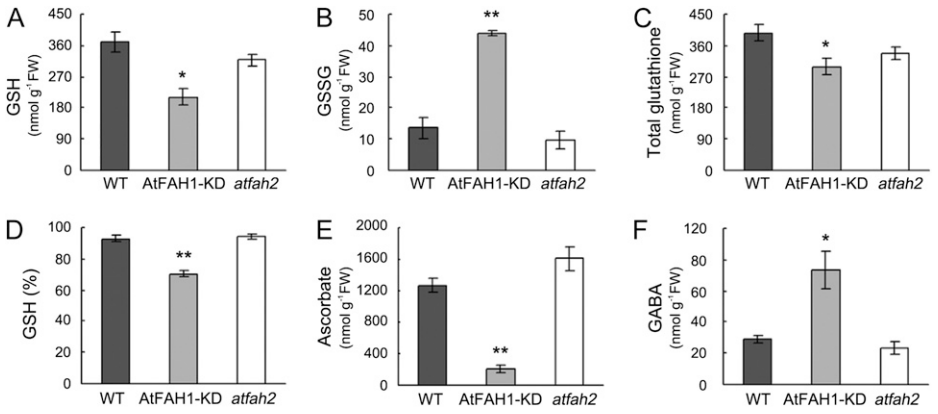

Figure 7. Profiling of oxidative-stress-related metabolites. Metabolites were extracted from 3-week-old wild-type, AtFAH1-KD, and *atfah2* plants, and analyzed by CE-MS. A, GSH. B, GSSG. C, Total glutathione. D, Ratio of GSH in total glutathione. E, Reduced ascorbate. F, GABA. Data are mean ± SE of three biological samples. $*P < 0.05$, $**P < 0.01$, compared with wild type (*t* test).

AtFAH1, and strongly support the significance of AtFAH1 in AtBI-1-mediated cell death regulation (Fig. 9).

DISCUSSION

Importance of AtCb5 in AtFAH Activity

It has been reported that ScFAH1 and mammalian FA2H contain a Cb5-like domain at their N terminus, and that the truncated FA2H lacking the Cb5-like domain has only a low level of FAH activity, indicating that the Cb5-like domain is required for efficient hydroxylation activity (Mitchell and Martin, 1997; Alderson et al., 2004). However, the Arabidopsis AtFAH1 and AtFAH2 lack the Cb5-like domain. This study demonstrated that both AtFAH1 and AtFAH2 were activated by AtCb5-B through their interaction.

In Arabidopsis, there are five Cb5s (AtCb5-A to -E), and AtCb5-B, -C, -D, and -E localized in the ER membrane (Maggio et al., 2007; Nagano et al., 2009). Cb5 is a ubiquitous eukaryotic electron transfer protein, and is related to a number of ER-linked redox enzyme systems such as hydroxylation, desaturation, and elongation (Mathews, 1985; Schenkman and Jansson, 2003). In addition, AtFAHs also possess several His motifs to receive electrons like ScFAH1 and FA2H. Therefore, AtFAHs would also need electrons from ER-localized Cb5 to work sufficiently, although there is a great difference among them in existence or lack of the Cb5-like domain.

Fatty Acid 2-Hydroxylation through AtFAH1 and AtFAH2 in Arabidopsis

Mammalian FA2H had no substrate specificity because *FA2H* is a single gene and the protein can generate almost all kinds of 2-HFAs when overexpressed (Alderson et al., 2004). However, analysis of 2-HFAs in Arabidopsis demonstrated that AtFAH1 2-hydroxylated all kinds of fatty acid, especially VLCFA, whereas AtFAH2 2-hydroxylated only palmitic acid in Arabidopsis cells. This finding suggests that

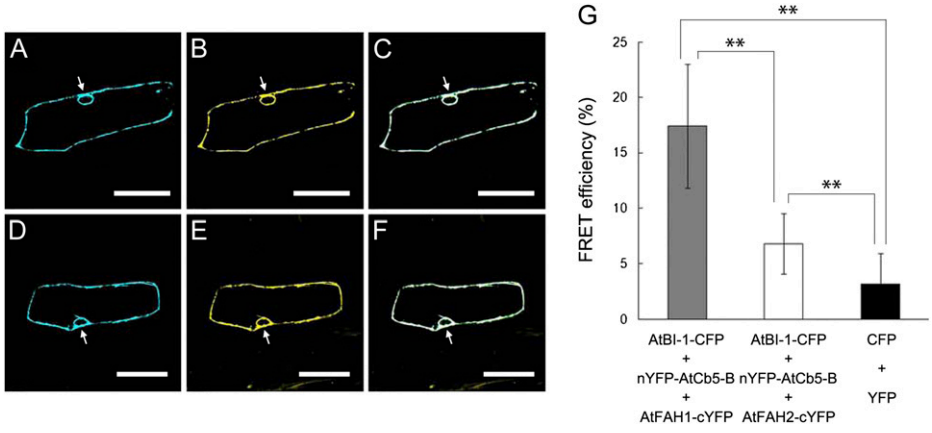

Figure 8. Detection of ternary interactions among AtBI-1, AtCb5-B, and AtFAH. A to F, Distribution of AtBI-1-CFP (A and D), nYFP-AtCb5-B/AtFAH1-cYFP (B), and nYFP-AtCb5-B/AtFAH2-cYFP (E). Onion epidermal cells transiently coexpressing the combination of AtBI-1-CFP, nYFP-AtCb5-B, and AtFAH1-cYFP or the combination of AtBI-1-CFP, nYFP-AtCb5-B, and AtFAH2-cYFP were examined by confocal laser-scanning microscopy. The merged image of A and B is shown in C, and the merged image of D and E is shown in F. Scale bars = 100 μm. Arrows indicate the perinuclear region. G, FRET-acceptor photobleaching analysis of the interactions between AtBI-1-CFP and nYFP-AtCb5-B/AtFAH1-cYFP or nYFP-AtCb5-B/AtFAH2-cYFP. Data are mean ± SD of FRET efficiency of 30 sample sites. $**P < 0.01$.

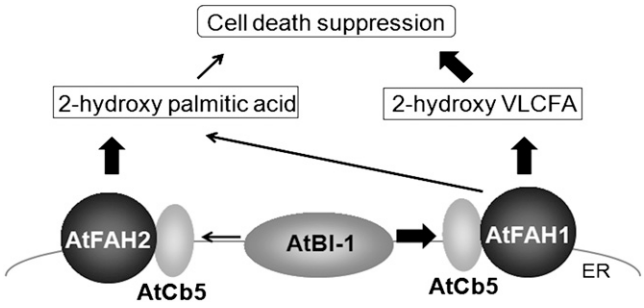

Figure 9. Schematic model of the relationship among AtBI-1, AtFAH, and cell death suppression. AtBI-1 interacts with AtFAH1 via AtCb5 more strongly than AtFAH2. 2-Hydroxy VLCFA, which is synthesized by AtFAH1, is positively related to cell death suppression. In contrast, 2-hydroxy palmitic acid, which is synthesized by AtFAH2 and marginally AtFAH1, comparatively has only a little participation in cell death suppression mediated by AtBI-1.

AtFAH1 and AtFAH2 are used differently depending on the length of fatty acids in Arabidopsis.

The synthetic pathway of VLCFA is quite different from that of long-chain fatty acid (LCFA). LCFAs, such as palmitic acid and stearic acid, are produced in plastids, whereas VLCFAs are generated in the ER membrane by a special elongase system comprising a four-step reaction cycle: condensation by 3-ketoacyl-CoA synthase; reduction by 3-ketoacyl-CoA reductase; dehydration by 3-hydroxyacyl-CoA dehydratase; and further reduction by trans-2-enoyl-CoA reductase (Bach and Faure, 2010). Therefore, it may be reasonable that the substrates of AtFAHs are differentiated between LCFA and VLCFA in Arabidopsis cells.

However, there might be no substrate specificity between AtFAH1 and AtFAH2, because the complementation assay showed that AtFAH2 could produce 26h:0 in yeast cells. One can speculate that VLCFAs are not supplied into AtFAH2 as substrates in Arabidopsis cells, although AtFAH2 could 2-hydroxylate VLCFAs. Alternatively, AtFAH1 might be associated also with the elongase system in the ER membrane of Arabidopsis cells. Further studies are needed to investigate the relationship between AtFAHs and elongase system or transportation of fatty acids. In addition, it is interesting to examine substrate specificities of AtFAHs in vitro.

On the other hand, above differentiation in Arabidopsis might not be applicable to other plants such as *Oryza sativa* and *Zea mays*, because they have only a few 2-hydroxy LCFAs, including 2-hydroxy palmitic acid in spite of possessing two FAH homologs (Imai et al., 1995; Pata et al., 2010). Therefore, it is also interesting to analyze the substrate of FAHs in a large number of plants and understand their differences.

The Relationship between AtFAH and AtBI-1 in Cell Death Suppression

Our previous studies showed that AtBI-1 required FAH function to suppress cell death, implying that sphingolipids with 2-HFAs play an important role in cell death regulation (Nagano et al., 2009). In this study, AtFAH1-KD and *atfah2* plants were more sensitive to H_2O_2 and MD than wild type, suggesting that 2-HFAs provide tolerance to oxidative stress, regardless of their length.

2-HFAs are considered to function as a part of sphingolipids, because they are mostly contained within sphingolipids in higher plants. A number of previous studies demonstrated the relationship between sphingolipids and cell death regulation in not only animals but also plants (Taha et al., 2006; Hannun and Obeid, 2008; Pata et al., 2010). Focused on the sphingolipid fatty acids, non-HFA ceramide induces apoptosis, whereas 2-HFA ceramide is less proapoptotic in mammalian U937 cells (Ji et al., 1995). In addition, Uchida et al. (2007) proposed that 2-hydroxylation of sphingolipid fatty acids can protect mammalian keratinocytes from apoptosis. In keratinocytes, 2-HFA ceramide and 2-HFA glucosylceramide are markedly increased during differentiation. Interestingly, differentiated keratinocytes are more resistant to apoptosis induced by ultraviolet irradiation and by tumor necrosis factor related apoptosis-inducing ligands (Chaturvedi et al., 1999; Magnoni et al., 2002; Jansen et al., 2003; Uchida et al., 2003). Similarly, the uptake of 2-HFA ceramide did not affect programmed cell death in Arabidopsis suspension cells, whereas non-HFA ceramide as well as C2-ceramide induced cell death (Townley et al., 2005). Therefore, 2-HFA sphingolipids may be important to cell death suppression or stress resistance in plant cells.

On the other hand, oxidative stress induced a rapid increase in *AtFAH1* mRNA and production of a large amount of 2-hydroxy VLCFAs. In addition, knockdown of *AtFAH1* affected the amounts of oxidative-stress-related metabolites such as ascorbate, glutathione, and GABA. Moreover, the BiFC-FRET assay demonstrated that AtFAH1 interacted with AtBI-1 via AtCb5-B more strongly than AtFAH2. These results are in agreement with our previous data that overexpression of *AtBI-1* in Arabidopsis is associated with increased 2-hydroxy VLCFAs (Nagano et al., 2009). These findings suggest that AtFAH1 is involved in AtBI-1 function more than AtFAH2, although *atfah2* are also hypersensitive to oxidative stress like AtFAH1-KD lines. It is possible that the presence of 16h:0 in the membranes of plant cells seems important, because the expression of *AtFAH2* mRNA were gradually decreased and no obvious changes were noted in the amount of 16h:0 and oxidative-stress-related metabolites in *atfah2* mutant. One can speculate that membrane permeability is probably enhanced in *atfah2* mutant. Further studies are necessary to clarify the difference in the effects of 2-HFA length on cell death regulation and the significance of 2-hydroxy VLCFA. In addition, 2-HFAs might be essential for plant development, because we could not obtain AtFAH1-KD/*atfah2* double mutants until now. We firmly believe that more vigorous efforts using AtFAH1 and AtFAH2 can shed more information on

the meaning of 2-HFA, because Arabidopsis has two functionally different FAHs.

MATERIALS AND METHODS

Plant Materials

The Columbia ecotype of Arabidopsis (*Arabidopsis thaliana*) was used in all experiments. The T-DNA insertion mutant of *AtFAH2* was obtained from the SALK Institute (SALK_011293). To generate AtFAH1-KD and *atfah2/pAtFAH2*::*AtFAH2* lines, pK7GWIWG2(II)-AtFAH1 and pMDC99-AtFAH2 were constructed, respectively. Briefly, the 3′-untranslated region of AtFAH1-cDNA (amplified by the primers: 5′-ACAAAAGCCCCCAGAAAAGA-3′ and 5′-AGAAGGATGATTAATAACT-3′), or putative native promoter and gene region of *AtFAH2* (amplified by the primers: 5′-GTGGAAAGCCTCATTGCTATATC-3′ and 5′-GGGAATCAAAGAAAAGTGAAATC-3′) were introduced into the pK7GWIWG2(II) or pMDC99 plasmids, respectively (Karimi et al., 2002; Curtis and Grossniklaus, 2003), by the Gateway system. The resulting plasmid was transferred to *Agrobacterium tumefaciens* strain EHA105 (Hood et al., 1993) using the freeze-thaw method (An et al., 1998). Transformations of Arabidopsis plants were carried out by the floral-dip method (Bechtold and Pelletier, 1998). Arabidopsis plants were cultivated at 23°C under continuous light (60 μmol m^{-2} s^{-1}).

Cytological Analysis of AtFAH1 and AtFAH2

GFP fusion protein with AtFAH1 (amplified by the primers: 5′-ATGGTTGCTCAGGGATTCAC-3′ and 5′-TTGCTCTTTTCTGGGGGCTT-3′) was prepared by amplification of the *AtFAH1* open reading frame without the stop codon. PCR product was introduced into the pEarley-gate 103 (Earley et al., 2006) by the Gateway system to generate the GFP C-terminal fusion construct, AtFAH1-GFP. Similarly, AtFAH2 (amplified by the primers: 5′-ATGGTTGCAGAACGATACAC-3′ and 5′-GCTCTTCTTCGCAGCGGCTTTAATA-3′) fusion protein with RFP at its C terminus was generated using the destination vector pK2GW7-TagRFP, which was kindly provided by Dr. Doniwa (University of Tokyo). The plasmid DNA was introduced into onion (*Allium cepa*) epidermal cells by particle bombardment with two helium-driven particle accelerators (PDS/1000; Bio-Rad or GIE-3 IDERA; TANAKA), as described by Arimura and Tsutsumi (2002) and Takahashi et al. (2006), respectively. Confocal laser microscopy was carried out with Nikon TE-2000U or Leica TCS-SP5. In both systems, a 488-nm Ar/Kr laser was used for the excitation of GFP. A 543-nm He/Ne laser was also used for RFP. Emission signals were detected using 515/30-nm filter for GFP, and a 590/70-nm or 570-nm long-pass filter for RFP.

BiFC Assay

Plasmids for BiFC analysis were kindly provided by Dr. Nakagawa (Shimane University). *AtFAH1* and *AtFAH2* open reading frames without their stop codons were combined with the BiFC destination vector cYFP-pUGW2 (Nakagawa et al., 2007) by the Gateway system to generate the cYFP (175–239 amino acids) C-terminal fusion constructs, AtFAH1-cYFP and AtFAH2-cYFP, respectively. Similarly, nYFP-AtCb5-B (amplified by the primers: 5′-ATGGGAGACGAAGCAAAGA-3′ and 5′-CCCTGATTTGGTGTAGATACGGATT-3′) fusion protein with nYFP (1–174 amino acids) at its N terminus was generated using the destination vector nYFP-pUGW0 (Nakagawa et al., 2007). The mixed plasmid DNA was introduced into onion epidermal cells by particle bombardment with helium-driven particle accelerator (GIE-3 IDERA; TANAKA). The CaMV35S-DsRed was also cobombarded to the cells as an expression marker. The BiFC signal was analyzed by fluorescence microscopy (DMRD; Leica) and confocal laser microscopy (TCS-SP5; Leica). In the latter system, a 514-nm Ar laser was used for the excitation of YFP. A 543-nm He/Ne laser was also used for DsRed. Emission signals were detected using a 515/30-nm filter for YFP, and a 590/70-nm or 570-nm long-pass filter for DsRed.

BiFC-FRET Assay

The CFP-fused construct and pair constructs for BiFC as a donor and an acceptor for FRET, respectively, were introduced into onion epidermal cells by particle bombardment with a helium-driven particle accelerator (PDS/1000; Bio-Rad). Confocal microscopy was carried out with Leica TCS-SP5. For FRET measurements, Leica FRET acceptor photobleaching was used according to the instructions provided by the manufacturer. EYFP was photobleached in a region 4 to 8 μm in diameter, by two to five scans with 514-nm laser at 100%. ECFP fluorescence intensity was quantified [before donor (d1)] and [after donor (d2)] acceptor photobleaching along the background fluorescence intensity (bk), and FRET efficiency was determined using the equation: $\{[(d2 - bk) - (d1 - bk)]/(d2 - bk)\}$.

Oxidative Stress Treatment

For measurement of ion leakage and chlorophyll content, and for RT-PCR analysis under oxidative stress condition, three leaf discs (5.5 mm in diameter) obtained from 3-week-old Arabidopsis plants were submerged in 1 mL of distilled water. After adding H_2O_2 or MD (Sigma) to become 100 mM or 60 μm, respectively, the leaf discs were vacuumed for 5 min. The floating discs were incubated at 23°C under continuous light (60 μmol m^{-2} s^{-1}) without shaking for several times.

For fatty acid analysis, 250 mg of whole rosettes of Arabidopsis were submerged in 20 mL of 100 mM H_2O_2 (Wako), which was diluted with distilled water, for 24 h, and washed in distilled water before extraction of total lipids.

RT-PCR

Total RNA was extracted from Arabidopsis leaf discs of seedlings using the RNeasy plant mini prep kit (Qiagen) and 1 μg was used as a template for RT-PCR with specific primers for *AtFAH1* (amplified by the primers: 5′-ATGGTTGCTCAGGGATTCAC-3′ and 5′-TTGCTCTTTTCTGGGGGCTT-3′), *AtFAH2* (amplified by the following primers: 5′-ATGGTTGCAGAACGATACAC-3′ and 5′-GCTCTTCTTCGCAGCGGCTT-3′), *AtBI-1* (amplified by the primers: 5′-ATGGATGCGTTCTCTTCCTTC-3′ and 5′-GTTTCTCCTTTTCTTCTTCT-3′), *Actin2* (amplified by the primers: 5′-GAGATTCACATGCCCAGAAGTCTTG-3′ and 5′-ACCTGCCTCATCATACTCGGC-3′), and *Actin8* (amplified by the primers: 5′-TGAGCCAGTCTTCATCGTC-3′ and 5′-TCTCTTGCTCGTAGTCGACA-3′). The conditions for direct amplification with Ready-to-Go RT-PCR beads (GE Health Care) were one cycle at 42°C for 25 min and 95°C for 5 min; 25 cycles at 95°C for 30 s, at 55°C for 30 s, and at 72°C for 1 min.

Yeast Strain and Lipid Extraction

The yeast (*Saccharomyces cerevisiae*) gene disruption mutant (Δ*fah1*) was purchased from Euroscarf. Plasmid vectors for overexpression in yeast cells were kindly provided by Dr. Ralph Panstruga and Dr. I.E. Somssich. To generate pMet-AtFAH1 and pMet-AtFAH2, *AtFAH1* and *AtFAH2* open reading frames with their stop codons were combined with the destination vector pMet-Cub-Ura3 by the Gateway system, respectively. The construction of pMet-ScFAH1 was described in our previous work (Nagano et al., 2009). The PCR-amplified coding region of *AtCb5-B* with the stop codon (amplified by the primers: 5′-CGGGATCCATGGGAGACGAAGCAAAGA-3′ and 5′-CGGGATCCCCCTGATTTGGTGTAGATAC-3′) was introduced into the *Bam*HI site of pACT2 vector (Clontech) to generate pACT2-AtCb5-B.

Wild-type (BY4741) cells and Δ*fah1* mutants were transformed, and the transformant cells were cultured in liquid medium for 1 d. Total lipids in each transformant were extracted according to the method described previously (Folch et al., 1957). 2-HFA methyl esters with 2-hydroxy pentadecanoic acid (15h:0) methyl ester as an internal standard were prepared and separated by silica gel TLC using *n*-hexane/diethyl ether (4:1, vol/vol) as the mobile phase, as described by Imai et al. (2000).

Plant Lipid Extraction

Total lipids including sphingolipids were extracted from whole rosettes of Arabidopsis (300 mg fresh weight) according to the method described by Markham et al. (2006). Total other lipids mainly including nonhydroxyl fatty acids were extracted from rosettes of Arabidopsis (1 g fresh weight) according to the method described by Bligh and Dyer (1959).

Fatty Acid Analysis

2-HFA methyl esters with 15h:0 methyl ester as an internal standard, or non-HFA methyl esters with margaric acid (17:0) methyl ester as an internal standard were prepared and separated by silica gel TLC using *n*-hexane/diethyl ether (4:1, vol/vol) as the mobile phase as described by Imai et al. (2000).

Derivatized 2-HFA samples were analyzed by GC (GC-2010, Shimadzu Scientific) as described by Nagano et al. (2009).

Similarly, derivatized non-HFA samples were analyzed by GC with the injector set in split mode. The analytes were fractionated on a Restek RTX-5 column (5% diphenyl polysiloxane, 95% dimethyl polysiloxane; 0.25 mm i.d., 0.25 μm D.F., 30 m), and the injection port and the transfer line were maintained at 250°C. The column temperature was programmed from 100°C (2-min hold) to 280°C at 4°C/min and maintained at 280°C for another 30 min. The absolute values of non-HFA were computed like those of 2-HFA as described by Nagano et al. (2009).

Ion Leakage Measurement

Electrolyte leakage was monitored using an electrical conductivity meter (Horiba, B-173) at several time points, and expressed as a relative value against total ion leakage, which was measured in the autoclaved samples (Kawai-Yamada et al., 2009).

Measurement of Chlorophyll Content

Three leaf discs from 3-week-old plants treated with various chemicals were soaked overnight in 1 mL of dimethyl formamide at 4°C. The chlorophyll content of the extract was then determined spectrophotometrically as described previously (Porra et al., 1989).

Analysis of Various Metabolites

For measurements using CE-MS, metabolites were extracted using methanol-MilliQ water (1:1) as described by Sato et al. (2004). Leaf samples were obtained, immediately frozen in liquid nitrogen, and stored at −80°C until further analysis. The metabolites were extracted by rapid grinding of tissues in liquid nitrogen followed by immediate addition of 10 volumes of ice-cooled methanol (10 μL mg^{-1} fresh weight) including 50 μM internal standards; Met sulfone was mixed by a vortex mixer for 1 min at 4°C and equal volume of Milli-Q water was added to the sample mixture. After centrifugation for 5 min at 15,000*g*, the supernatant was ultrafiltrated through a 5-kD cutoff filter (Amicon). The filtrate was analyzed using the CE-MS method.

Separation and determination of metabolites were performed using the CE/MS system (Agilent Technologies). For the determination of anionic compounds, separations were carried out using fused-silica capillary (50 μm i.d. × 80 cm total length) filled with 50 mM ammonium acetate (pH 9.0) as the electrolyte according to the pressure-assisted CE-MS method (Harada et al., 2006). Cationic compounds were separated in an uncoated fused-silica capillary (50 μm i.d. × 100 cm total length) using 1 M formic acid (pH 1.9) as the electrolyte (Soga and Heiger, 2000; Miyagi et al., 2010; Takahara et al., 2010).

Sequence data from this article can be found in the Arabidopsis Genome Initiative or GeneBank/EMBL databases under the following accession numbers: AtFAH1, At2g34770; AtFAH2, At4g20870; AtCb5-B, At2g32720; AtBI-1, At5g47120.

ACKNOWLEDGMENTS

Plasmids used for the yeast assay were generously provided by Dr. Ralph Panstruga (Max-Planck Institute, Saabruecken, Germany) and Dr. Imer E. Somssich (Max-Planck Institute). Plasmids used for the BiFC assay were kindly provided by Dr. Tsuyoshi Nakagawa (Shimane University, Japan). pK2GW7-TagRFP was kindly provided by Dr. Yoko Doniwa (University of Tokyo, Japan). We appreciate Dr. Noriko Inada (Nara Institute of Science and Technology, Japan) for technical advice of confocal laser microscopy and BiFC-FRET. We are grateful to Dr. Hiroyuki Imai (Konan University, Japan) for his advice about fatty acid analysis and sphingolipids. We thank the members of the Laboratory of Cellular Functions at the University of Tokyo for technical assistance, comments, and participation in discussions.

Received May 1, 2012; accepted May 17, 2012; published May 25, 2012.

LITERATURE CITED

Alderson NL, Hama H (2009) Fatty acid 2-hydroxylase regulates cAMP-induced cell cycle exit in D6P2T schwannoma cells. J Lipid Res **50:** 1203–1208

Alderson NL, Maldonado EN, Kern MJ, Bhat NR, Hama H (2006) FA2H-dependent fatty acid 2-hydroxylation in postnatal mouse brain. J Lipid Res **47:** 2772–2780

Alderson NL, Rembiesa BM, Walla MD, Bielawska A, Bielawski J, Hama H (2004) The human FA2H gene encodes a fatty acid 2-hydroxylase. J Biol Chem **279:** 48562–48568

Alderson NL, Walla MD, Hama H (2005) A novel method for the measurement of in vitro fatty acid 2-hydroxylase activity by gas chromatography-mass spectrometry. J Lipid Res **46:** 1569–1575

An G, Ebert RR, Mitra A, Ha SB (1998) Binary vectors. *In* SB Gelvin, RA Schiperoort, eds, Plant Molecular Biology Manual. Kluwer Academic Publishers, Dordrecht, The Netherlands, pp 1–19

Arimura S, Tsutsumi N (2002) A dynamin-like protein (ADL2b), rather than FtsZ, is involved in Arabidopsis mitochondrial division. Proc Natl Acad Sci USA **99:** 5727–5731

Bach L, Faure JD (2010) Role of very-long-chain fatty acids in plant development, when chain length does matter. C R Biol **333:** 361–370

Bechtold N, Pelletier G (1998) In planta Agrobacterium-mediated transformation of adult Arabidopsis thaliana plants by vacuum infiltration. Methods Mol Biol **82:** 259–266

Bligh EG, Dyer WJ (1959) A rapid method of total lipid extraction and purification. Can J Biochem Physiol **37:** 911–917

Bouché N, Fromm H (2004) GABA in plants: just a metabolite? Trends Plant Sci **9:** 110–115

Chaturvedi V, Qin JZ, Denning MF, Choubey D, Diaz MO, Nickoloff BJ (1999) Apoptosis in proliferating, senescent, and immortalized keratinocytes. J Biol Chem **274:** 23358–23367

Curtis MD, Grossniklaus U (2003) A gateway cloning vector set for high-throughput functional analysis of genes in planta. Plant Physiol **133:** 462–469

Dunn TM, Lynch DV, Michaelson LV, Napier JA (2004) A post-genomic approach to understanding sphingolipid metabolism in *Arabidopsis thaliana*. Ann Bot (Lond) **93:** 483–497

Earley KW, Haag JR, Pontes O, Opper K, Juehne T, Song K, Pikaard CS (2006) Gateway-compatible vectors for plant functional genomics and proteomics. Plant J **45:** 616–629

Folch J, Lees M, Sloane Stanley GH (1957) A simple method for the isolation and purification of total lipides from animal tissues. J Biol Chem **226:** 497–509

Hama H (2010) Fatty acid 2-hydroxylation in mammalian sphingolipid biology. Biochim Biophys Acta **1801:** 405–414

Hannun YA, Obeid LM (2008) Principles of bioactive lipid signalling: lessons from sphingolipids. Nat Rev Mol Cell Biol **9:** 139–150

Harada K, Fukusaki E, Kobayashi A (2006) Pressure-assisted capillary electrophoresis mass spectrometry using combination of polarity reversion and electroosmotic flow for metabolomics anion analysis. J Biosci Bioeng **101:** 403–409

Hood EE, Gelvin SB, Melchers LS, Hoekema A (1993) New Agrobacterium vector for plant transformation. Transgenic Res **2:** 208–218

Ihara-Ohori Y, Nagano M, Muto S, Uchimiya H, Kawai-Yamada M (2007) Cell death suppressor Arabidopsis bax inhibitor-1 is associated with calmodulin binding and ion homeostasis. Plant Physiol **143:** 650–660

Imai H, Ohnishi M, Kinishita M, Kojima M, Ito S (1995) Structure and distribution of cerebroside containing unsaturated hydroxyl fatty acids in plant leaves. Biosci Biotechnol Biochem **59:** 1309–1313

Imai H, Yamamoto K, Shibahara A, Miyatani S, Nakayama T (2000) Determining double-bond positions in monoenoic 2-hydroxy fatty acids of glucosylceramides by gas chromatography-mass spectrometry. Lipids **35:** 233–236

Ishikawa T, Takahara K, Hirabayashi T, Matsumura H, Fujisawa S, Terauchi R, Uchimiya H, Kawai-Yamada M (2010) Metabolome analysis of response to oxidative stress in rice suspension cells overexpressing cell death suppressor Bax inhibitor-1. Plant Cell Physiol **51:** 9–20

Jansen BJ, van Ruissen F, Cerneus S, Cloin W, Bergers M, van Erp PE, Schalkwijk J (2003) Tumor necrosis factor related apoptosis inducing ligand triggers apoptosis in dividing but not in differentiating human epidermal keratinocytes. J Invest Dermatol **121:** 1433–1439

Ji L, Zhang G, Uematsu S, Akahori Y, Hirabayashi Y (1995) Induction of apoptotic DNA fragmentation and cell death by natural ceramide. FEBS Lett **358:** 211–214

Karimi M, Inzé D, Depicker A (2002) GATEWAY vectors for *Agrobacterium*-mediated plant transformation. Trends Plant Sci **7:** 193–195

Kawai-Yamada M, Hori Z, Ogawa T, Ihara-Ohori Y, Tamura K, Nagano M, Ishikawa T, Uchimiya H (2009) Loss of calmodulin binding to Bax inhibitor-1 affects Pseudomonas-mediated hypersensitive response-associated cell death in *Arabidopsis thaliana*. J Biol Chem **284:** 27998–28003

Kawai-Yamada M, Jin L, Yoshinaga K, Hirata A, Uchimiya H (2001) Mammalian Bax-induced plant cell death can be down-regulated by overexpression of Arabidopsis Bax Inhibitor-1 (AtBI-1). Proc Natl Acad Sci USA **98:** 12295–12300

Kawai-Yamada M, Ohori Y, Uchimiya H (2004) Dissection of *Arabidopsis* Bax inhibitor-1 suppressing Bax-, hydrogen peroxide-, and salicylic acid-induced cell death. Plant Cell **16:** 21–32

Kinnersley AM, Turano FJ (2000) Gamma aminobutyric acid (GABA) and plant responses to stress. Crit Rev Plant Sci **19:** 479–509

Kwaaitaal M, Keinath NF, Pajonk S, Biskup C, Panstruga R (2010) Combined bimolecular fluorescence complementation and Forster resonance energy transfer reveals ternary SNARE complex formation in living plant cells. Plant Physiol **152:** 1135–1147

Maggio C, Barbante A, Ferro F, Frigerio L, Pedrazzini E (2007) Intracellular sorting of the tail-anchored protein cytochrome *b5* in plants: a comparative study using different isoforms from rabbit and *Arabidopsis*. J Exp Bot **58:** 1365–1379

Magnoni C, Euclidi E, Benassi L, Bertazzoni G, Cossarizza A, Seidenari S, Giannetti A (2002) Ultraviolet B radiation induces activation of neutral and acidic sphingomyelinases and ceramide generation in cultured normal human keratinocytes. Toxicol In Vitro **16:** 349–355

Maier H, Meixner M, Hartmann D, Sandhoff R, Wang-Eckhardt L, Zöller I, Gieselmann V, Eckhardt M (2011) Normal fur development and sebum production depends on fatty acid 2-hydroxylase expression in sebaceous glands. J Biol Chem **286:** 25922–25934

Maldonado EN, Alderson NL, Monje PV, Wood PM, Hama H (2008) FA2H is responsible for the formation of 2-hydroxy galactolipids in peripheral nervous system myelin. J Lipid Res **49:** 153–161

Markham JE, Li J, Cahoon EB, Jaworski JG (2006) Separation and identification of major plant sphingolipid classes from leaves. J Biol Chem **281:** 22684–22694

Mathews FS (1985) The structure, function and evolution of cytochromes. Prog Biophys Mol Biol **45:** 1–56

Mehlhorn H, Lelandais M, Korth HG, Foyer CH (1996) Ascorbate is the natural substrate for plant peroxidases. FEBS Lett **378:** 203–206

Mitchell AG, Martin CE (1997) Fah1p, a *Saccharomyces cerevisiae* cytochrome b_5 fusion protein, and its *Arabidopsis thaliana* homolog that lacks the cytochrome b_5 domain both function in the alpha-hydroxylation of sphingolipid-associated very long chain fatty acids. J Biol Chem **272:** 28281–28288

Miyagi A, Takahashi H, Takahara K, Hirabayashi T, Nishimura Y, Tezuka T, Kawai-Yamada M, Uchimiya H (2010) Principal component and hierarchical clustering analysis of metabolites in destructive weeds; polygonaceous plants. Metabolomics **6:** 146–155

Nagano M, Ihara-Ohori Y, Imai H, Inada N, Fujimoto M, Tsutsumi N, Uchimiya H, Kawai-Yamada M (2009) Functional association of cell death suppressor, Arabidopsis Bax inhibitor-1, with fatty acid 2-hydroxylation through cytochrome b_5. Plant J **17:** 122–134

Nakagawa T, Suzuki T, Murata S, Nakamura S, Hino T, Maeo K, Tabata T, Kawai T, Tanaka K, Niwa Y, Watanabe Y, et al (2007) Improved Gateway binary vectors: high-performance vectors for creation of fusion constructs in transgenic analysis of plants. Biosci Biotechnol Biochem **71:** 2095–2100

Nakano Y, Asada K (1987) Purification of ascorbate peroxidase in spinach chloroplasts: its inactivation in ascorbate-depleted medium and reactivation by monodehydroascorbate radical. Plant Cell Physiol **28:** 131–140

Noctor G, Foyer CH (1998) Ascorbate and glutathione: keeping active oxygen under control. Annu Rev Plant Physiol Plant Mol Biol **49:** 249–279

Oh CS, Toke DA, Mandala S, Martin CE (1997) ELO2 and ELO3, homologues of the *Saccharomyces cerevisiae* ELO1 gene, function in fatty acid elongation and are required for sphingolipid formation. J Biol Chem **272:** 17376–17384

Pata MO, Hannun YA, Ng CK-Y (2010) Plant sphingolipids: decoding the enigma of the Sphinx. New Phytol **185:** 611–630

Porra RJ, Thompson WA, Kriedemann PE (1989) Determination of accurate extinction coefficients and simultaneous equations for assaying chlorophylls *a* and *b* extracted with four different solvents: verification of the concentration of chlorophyll standards by atomic absorption spectroscopy. Biochim Biophys Acta **975:** 384–394

Raffaele S, Leger A, Roby D (2009) Very long chain fatty acid and lipid signaling in the response of plants to pathogens. Plant Signal Behav **4:** 94–99

Sato S, Soga T, Nishioka T, Tomita M (2004) Simultaneous determination of the main metabolites in rice leaves using capillary electrophoresis mass spectrometry and capillary electrophoresis diode array detection. Plant J **40:** 151–163

Schenkman JB, Jansson I (2003) The many roles of cytochrome b_5. Pharmacol Ther **97:** 139–152

Schneider SA, Bhatia KP (2010) Three faces of the same gene: FA2H links neurodegeneration with brain iron accumulation, leukodystrophies, and hereditary spastic paraplegias. Ann Neurol **68:** 575–577

Shyu YJ, Suarez CD, Hu CD (2008a) Visualization of AP-1 NF-kappaB ternary complexes in living cells by using a BiFC-based FRET. Proc Natl Acad Sci USA **105:** 151–156

Shyu YJ, Suarez CD, Hu CD (2008b) Visualization of ternary complexes in living cells by using a BiFC-based FRET assay. Nat Protoc **3:** 1693–1702

Soga T, Heiger DN (2000) Amino acid analysis by capillary electrophoresis electrospray ionization mass spectrometry. Anal Chem **72:** 1236–1241

Taha TA, Mullen TD, Obeid LM (2006) A house divided: ceramide, sphingosine, and sphingosine-1-phosphate in programmed cell death. Biochim Biophys Acta **1758:** 2027–2036

Takahara K, Kasajima I, Takahashi H, Hashida SN, Itami T, Onodera H, Toki S, Yanagisawa S, Kawai-Yamada M, Uchimiya H (2010) Metabolome and photochemical analysis of rice plants overexpressing Arabidopsis NAD kinase gene. Plant Physiol **152:** 1863–1873

Takahashi H, Toyoda K, Hirakawa Y, Morishita K, Kato T, Inagaki Y, Ichinose I, Shiraishi T (2006) Localization and responsiveness of a cowpea apyrase VsNTPase1 to phytopathogenic microorganisms. J Gen Plant Pathol **72:** 143–151

Taoka K, Ohki I, Tsuji H, Furuita K, Hayashi K, Yanase T, Yamaguchi M, Nakashima C, Purwestri YA, Tamaki S, et al (2011) 14-3-3 proteins act as intracellular receptors for rice Hd3a florigen. Nature **476:** 332–335

Townley HE, McDonald K, Jenkins GI, Knight MR, Leaver CJ (2005) Ceramides induce programmed cell death in *Arabidopsis* cells in a calcium-dependent manner. Biol Chem **386:** 161–166

Uchida Y, Hama H, Alderson NL, Douangpanya S, Wang Y, Crumrine DA, Elias PM, Holleran WM (2007) Fatty acid 2-hydroxylase, encoded by FA2H, accounts for differentiation-associated increase in 2-OH ceramides during keratinocyte differentiation. J Biol Chem **282:** 13211–13219

Uchida Y, Nardo AD, Collins V, Elias PM, Holleran WM (2003) De novo ceramide synthesis participates in the ultraviolet B irradiation-induced apoptosis in undifferentiated cultured human keratinocytes. J Invest Dermatol **120:** 662–669

Watanabe N, Lam E (2006) *Arabidopsis* Bax inhibitor-1 functions as an attenuator of biotic and abiotic types of cell death. Plant J **45:** 884–894

Watanabe N, Lam E (2008) Arabidopsis Bax inhibitor-1: a rheostat for ER stress-induced programmed cell death. Plant Signal Behav **3:** 564–566

Xu Q, Reed JC (1998) Bax inhibitor-1, a mammalian apoptosis suppressor identified by functional screening in yeast. Mol Cell **1:** 337–346

Yoshinaga K, Fujimoto M, Arimura S, Tsutsumi N, Uchimiya H, Kawai-Yamada M (2006) The mitochondrial fission regulator DRP3B does not regulate cell death in plants. Ann Bot (Lond) **97:** 1145–1149